The Plant Cell, Vol. 25: 2253–2264, June 2013, www.plantcell.org

Arabidopsis BPM Proteins Function as Substrate Adaptors to a CULLIN3-Based E3 Ligase to Affect Fatty Acid Metabolism in Plants[W]

Liyuan Chen,[a] Joo Hyun Lee,[a] Henriette Weber,[b] Takayuki Tohge,[c] Sandra Witt,[c] Sanja Roje,[d] Alisdair R. Fernie,[c] and Hanjo Hellmann[a,1]

[a] School of Biological Sciences, Washington State University, Pullman, Washington 99164
[b] Angewandte Genetik, Freie University, 14195 Berlin, Germany
[c] Max-Planck Institute for Molecular Plant Physiology, 14476 Golm, Germany
[d] Institute of Biological Chemistry, Washington State University, Pullman, Washington 99164

ORCID ID: 0000-0003-2177-2168 (H.H.).

Regulation of transcriptional processes is a critical mechanism that enables efficient coordination of the synthesis of required proteins in response to environmental and cellular changes. Transcription factors require accurate activity regulation because they play a critical role as key mediators assuring specific expression of target genes. In this work, we show that CULLIN3-based E3 ligases have the potential to interact with a broad range of ETHYLENE RESPONSE FACTOR (ERF)/APETALA2 (AP2) transcription factors, mediated by MATH-BTB/POZ (for Meprin and TRAF [tumor necrosis factor receptor associated factor] homolog)-Broad complex, Tramtrack, Bric-a-brac/Pox virus and Zinc finger) proteins. The assembly with an E3 ligase causes degradation of their substrates via the 26S proteasome, as demonstrated for the WRINKLED1 ERF/AP2 protein. Furthermore, loss of MATH-BTB/POZ proteins widely affects plant development and causes altered fatty acid contents in mutant seeds. Overall, this work demonstrates a link between fatty acid metabolism and E3 ligase activities in plants and establishes CUL3-based E3 ligases as key regulators in transcriptional processes that involve ERF/AP2 family members.

INTRODUCTION

Effective mechanisms that control the timing of developmental and physiological processes and regulate these processes in response to environmental cues are of utmost importance to plants due to their sessile lifestyle. One mechanism that allows plants to quickly and flexibly respond is the ubiquitin (UBQ) proteasome pathway (Hua and Vierstra, 2011). This pathway is highly conserved among eukaryotes and requires the concerted activities of an E1 UBQ activating enzyme, a UBQ conjugating enzyme E2, and an E3 UBQ ligase. While E1 and E2 activate the UBQ to modify target substrates, the E3 ligase binds the E2 and a substrate protein to facilitate transfer of the UBQ moiety. Upon building up a UBQ chain on the substrate, the ubiquitylated protein is marked for degradation via the 26S proteasome (Hua and Vierstra, 2011).

CULLIN3 (CUL3)-based Really Interesting New Gene (RING) E3 ligases (CRL3) have been described only recently and mainly with respect to their basic architecture (Figueroa et al., 2005; Gingerich et al., 2005, 2007; Weber et al., 2005). They are composed of a CUL3 protein, as the scaffolding subunit, that binds in its C-terminal region the RING-finger protein RING-Box protein 1 (RBX1), while its N-terminal part is recognized by proteins containing a BTB/POZ fold (Figueroa et al., 2005; Weber et al., 2005). BTB/POZ proteins comprise a diverse group of proteins within *Arabidopsis thaliana* and rice (*Oryza sativa*), containing 80 and 149 members, respectively (Gingerich et al., 2007). They have been divided into 12 subgroups based on their secondary domains (Gingerich et al., 2007). While the BTB/POZ fold is required for assembly with the cullin and to interact with other BTB/POZ proteins, the secondary domain may function as an adaptor to allow binding of a substrate and delivery to the CRL3 core for ubiquitylation.

Based on its role as the central scaffolding subunit that assembles with potentially many BTB/POZ proteins, it is not surprising that the loss of CUL3 causes an embryo-lethal phenotype. Reduced amounts of functional CUL3 protein affect red light and ethylene signaling and impair plant development (Dieterle et al., 2005; Thomann et al., 2009).

One BTB/POZ subfamily is the BTB/POZ-MATH (BPM) family, which contains a BTB/POZ fold in their C-terminal region and a MATH domain located within the first 200 amino acids of their N-terminal region. The family comprises six members in *Arabidopsis*, all of which have molecular masses between 40 and 50 kD (Weber et al., 2005). Recent findings indicate that substrates of BPM proteins, and, thus, of a corresponding $CRL3^{BPM}$ E3 ligase, are predominantly transcription factors, as assembly with RELATED TO APETALA2.4 (RAP2.4), a member of the ETHYLENE RESPONSE FACTOR/APETALA2 (ERF/AP2) family, and with HB6, a class I homeobox Leucine zipper transcription factor, have been reported (Weber and Hellmann, 2009; Lechner et al., 2011). While the role of BPM/RAP2.4 assembly remains elusive, the assembly with Homeobox protein 6 (HB6) appears

[1] Address correspondence to hellmann@wsu.edu.
The author responsible for distribution of materials integral to the findings presented in this article in accordance with the policy described in the Instructions for Authors (www.plantcell.org) is: Hanjo Hellmann (hellmann@wsu.edu).
[W] Online version contains Web-only data.
www.plantcell.org/cgi/doi/10.1105/tpc.112.107292

to be a critical step in abscisic acid (ABA) signaling (Lechner et al., 2011).

Here, we describe that *Arabidopsis* BPM proteins assemble widely with ERF/AP2 transcription factors, and we demonstrate with a selected member of this family, WRINKLED1 (WRI1), that the interaction is a requirement to destabilize WRI1 in plants. BPM proteins are largely necessary for normal development, and loss-of-function mutants affected in all six members are affected in metabolism and fatty acid content. The results provide in planta proof for $CRL3^{BPM}$ E3 ligase activity affecting one of the major plant-specific transcription factor families, thus emphasizing their central role in plant metabolism and physiology.

RESULTS

BPM Proteins Interact Broadly with ERF/AP2 Transcription Factors

We earlier described that BPM proteins assemble with several, but not all members, of the A6 group of ERF/AP2 transcription factors (Weber and Hellmann, 2009). According to Sakuma and coworkers, the ERF/AP2 superfamily can be divided into five subgroups: AP2, RELATED TO ABI3/VP1 (RAV), DEHYDRATION-RESPONSIVE ELEMENT BINDING (DREB), ERF, and others (Sakuma et al., 2002). The A6 group belongs to the ERF subfamily. To investigate how broadly BPM proteins assemble with ERF/AP2 transcription factors, we also tested additional members outside the A6 group in yeast two-hybrid (Y2H) assays using BPM1 as prey (Figure 1A). The ERF subfamily member ERF1 (At3g23240) showed weak interaction, while the ERF subfamily members WRINKLED1 (At3g54320) and ERF4 (At3g15210) showed a strong interaction with BPM1 in the Y2H assay. WRI1 also tested positively for self-assembly in the yeast assay (Figure 1B). Finally, DREB1a (At4g25480), which belongs to the DREB subfamily, as well as RAV1 (At1g13260), a member of the RAV subfamily, strongly interacted with BPM1 (Figure 1A). Since BPMs also interact with CUL3 proteins, we tested the interaction of the different ERF/AP2 transcription factors with CUL3a and did not observe any interaction in the yeast system. We therefore concluded that a large number of ERF/AP2 transcription factors are likely recognized by BPM proteins in *Arabidopsis*.

CUL3 and BPM Proteins Assemble in Planta with WRI1

To understand the basic principles of $CRL3^{BPM}$ complex assembly with substrates, we focused on a single well-described protein, WRI1, which is a key player in fatty acid and carbohydrate metabolism (Cernac and Benning, 2004; Baud et al., 2009).

In agreement with findings from the Y2H assays, pull-down experiments using a glutathione *S*-transferase (GST):WRI1 fusion protein demonstrated that this protein can coprecipitate in vitro–translated BPM1 from rabbit reticulolysates (Figure 1C). For further investigation of in planta complex assembly, specific peptide-based antibodies were raised against CUL3 and WRI1 (see Supplemental Figure 1 online). The antibody against CUL3 did not distinguish between CUL3a and b (see Supplemental Figures 1A and 1C online); however, transient expression experiments in *Nicotiana benthamiana* clearly demonstrated specificity of the α-CUL3 antibody. We only observed a single band of around 85 kD appearing on protein gel blots with wild-type or *cul3* mutant plant extracts (see Supplemental Figure 1B online). Likewise, only a single band was detectable when the α-WRI1 antibody was used on total plant extracts from wild-type plants, which was missing in a *wri1-3* mutant when the α-WRI1 antibody was used on total plant extracts (see Supplemental Figure 1E online).

Pull-down experiments using GST:WRI1 against wild-type plant extract showed that the fusion protein precipitates both endogenous WRI1 and CUL3; however, this was not the case with GST alone (Figure 1D). In addition, pull-down analysis with GST- and His-tag proteins expressed in and purified from *Escherichia coli* demonstrated that BPM proteins are necessary to bridge assembly between WRI1 and CUL3 proteins. Here, His:WRI1 is only capable of coprecipitating GST:CUL3a, if GST:BPM1 protein is present in the assay but not with GST alone (Figure 1F). Also, immunoprecipitation (IP) studies using the α-WRI1 antibody successfully precipitated CUL3 from plant extracts in the wild-type background (Figure 1G). We also observed comigration of WRI1 with CUL3 in fast protein liquid chromatography (FPLC) studies (see Supplemental Figure 2A online) and detected green fluorescent protein (GFP):WRI1 localized to the nucleus, as has been previously shown for most BPM proteins and CUL3a (see Supplemental Figure 2B online; Weber and Hellmann, 2009). Overall, these studies demonstrate that WRI1 assembles with CUL3 proteins in planta and support the working hypothesis that the assembly is mediated by BPM proteins.

WRI1 Is a CUL3-Dependent Target of the 26S Proteasome

One outcome of BPM assembly with CUL3 proteins is the proteolytic degradation of their substrates. Consequently, stability assays were performed using the translational inhibitor cycloheximide (CHX) and the proteasomal inhibitor MG132. In initial experiments, CHX treatments did not point to instability of the WRI1 protein (see Supplemental Figure 3A online), although accumulation of WRI1 was observed when plants were treated with MG132 (see Supplemental Figure 3A online).

To better understand this phenomenon, WRI1 expression was tested in plants treated with CHX or with the proteasomal inhibitor. While plants incubated with MG132 did not show any change in *WRI1* expression, CHX caused a strong upregulation of the *WRI1* gene (see Supplemental Figure 3B online). It was therefore decided to pretreat plants with the transcriptional inhibitor actinomycin D2 (ActD2) before CHX treatment. Under these conditions, WRI1 protein was completely gone after 6 h treatment, and its disappearance was blocked by coincubation with MG132 (Figure 2A), demonstrating that WRI1 is unstable in a 26S proteasome–dependent manner. Notably, the accumulation of WRI1 protein in samples treated with all three inhibitors is most likely due to pretreatment of plants with ActD2 and MG132 for 3 h before the addition of CHX.

A $cul3^{hyp}$ double mutant that was previously described is knocked out for CUL3b and partially functional for CUL3a (Thomann et al., 2009). We took advantage of this mutant to investigate whether WRI1 is stabilized in this genetic background

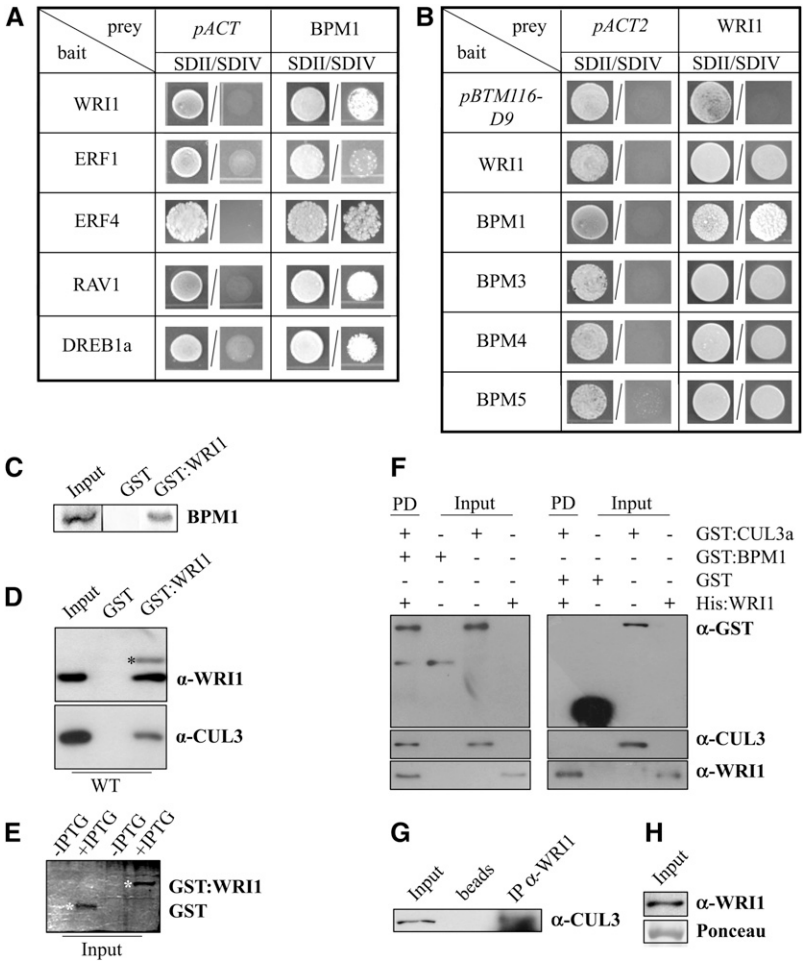

Figure 1. Interaction Studies of WRI1 with BPM and CUL3 Proteins.

(A) BPM1 interacts with ERF4, RAV1, and DREB1a, but only poorly with ERF1, in Y2H assays. SDII, medium for transformation selection; SDIV, medium for test of interaction. Pictures of single spots were taken 7 d after transformation.

(B) WRI1 can assemble with itself in Y2H assay, as well as with representative members of the BPM family, BPM1, BPM3, BPM4, and BPM5.

(C) In vitro–translated and [^{35}S]Met-labeled BPM1 protein was used in pull-down assay with *E. coli*–expressed GST and GST:WRI1.

(D) Pull-down experiments with *E. coli*–expressed GST:WRI1 results in the precipitation of WRI1 and CUL3, while GST alone was ineffective. Asterisks indicate GST:WRI1 band, while the band below is plant WRI1. Pulldowns were first tested with α-WRI1 and then with α-CUL3 after the membrane had been stripped. WT, the wild type.

(E) Silver-stained SDS-PAGE gel to illustrate the Isopropyl-β-D-thiogalactopyranosid (IPTG)-induced expression of purified GST and GST:WRI1 proteins from *E. coli*. Asterisks mark the bands of the corresponding proteins.

(F) Pull-down (PD) experiments with purified proteins show that His:WRI1 can precipitate GST:CUL3a if GST:BPM1 is present in the assay (left blot), while this is not the case when GST alone is used (right blot). Blots were first probed with an α-GST antibody, then stripped and subsequently probed with α-CUL3 and α-WRI1.

(G) IP experiments with α-WRI1 antibody shows coprecipitation of CUL3 with WRI1 from *Arabidopsis* wild-type protein extract. If not otherwise stated in this and subsequent figures, 30 μg of total protein extract was loaded as input, and experiments were done with 14-d-old seedlings.

(H) WRI1 is present in the plant extract used for the IP shown in **(G)**. Ponceau in this and all subsequent figures refers to unspecific staining of blotted proteins with Ponceau S and was used as a loading control. Results shown in this and all subsequent figures are based on at least three independent biological replicates.

and to prove that the instability is mediated by a CUL3-based complex. Protein gel blot analysis on wild-type and *cul3^{hyp}* plant extracts showed that WRI1 was present in the mutant in higher amounts than in the wild type (Figure 2B). This was not based on increased transcriptional activities in the mutant since no significant difference in *WRI1* expression was detectable in either plant (Figure 2C). Stability assays with ActD2 and CHX showed no considerable change in protein content in the mutant over a 6-h treatment period, while WRI1 was not detectable in wild-type extracts (Figure 2D), revealing that

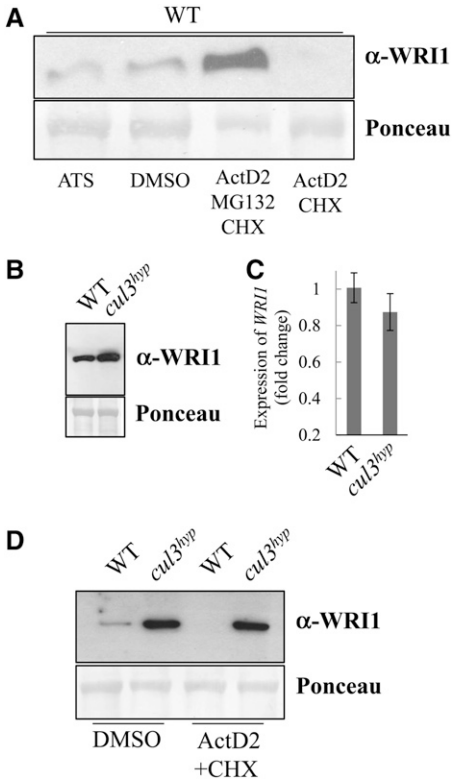

Figure 2. Stability and Expression Level of WRI1 in the Wild Type and *cul3^{hyp}*.

(A) Treatment of wild-type (WT) plants with ActD2 (6 h) and CHX (3 h) inhibitors shows instability of WRI1. This is blocked by cotreatment with MG132 (6 h).

(B) WRI1 protein accumulates in *cul3^{hyp}* double mutants in comparison to the wild type.

(C) Expression of *WRI1* is comparable to the wild type in *cul3^{hyp}* plants.

(D) WRI1 protein is more stable in *cul3^{hyp}* than in the wild type. Error bars in this and all subsequent figures represent SD.

WRI1 is unstable in a 26S proteasome– and CUL3-dependent manner.

BPM Proteins Bridge the Assembly between WRI1 and CUL3 and Are Broadly Important for Development

Our results strongly support the idea that BPM proteins assemble with a broad range of ERF/AP2 transcription factors and that, if ERF/AP2 proteins are in complex with CUL3s, the BPMs likely function as their bridging substrate receptors. Since WRI1 is unstable, and because complex formation requires presence of a functional CUL3 protein in the plant, it was necessary to investigate whether the loss of BPM proteins is also stabilizing WRI1.

Two strategies were followed to support the hypothesis that BPM proteins function as substrate receptors and are required for mediating WRI1 instability. First, because of a lack of T-DNA insertion mutants for nearly all *BPM* genes, a 35S artificial microRNA construct was designed to downregulate expression of all six members, based on predictions from the WMD 2 - Web MicroRNA Designer (http://wmd2.weigelworld.org) (the lines are further denoted as *6xamiBPM*). Second, the MATH domain from BPM1 was cloned under the control of a 35S promoter and behind a GFP reporter, and with (further denoted as *BPM1$^{MATH:NLS}$*) or without (*BPM1^{MATH}*) a nuclear localization signal attached to the end of the domain to affect subcellular localization. The MATH construct was generated to impose a competition in the plant where endogenous BPM proteins have reduced access to WRI1 and, thus, hypothetically cause its stabilization.

Several independent plant lines were successfully generated, and two independent lines of the T4 generation were chosen for each construct for further analysis. In both *6xamiBPM* lines, a significant downregulation in gene expression of all *BPMs* was measurable (Figures 3A and 3B), while the *BPM1^{MATH}* and *BPM1$^{MATH:NLS}$* lines showed strong expression of the transgene (Figure 3C). In addition, based on the GFP reporter, *BPM1^{MATH}* constructs were detectable throughout the cell, including the nucleus (see Supplemental Figure 4A online), while *BPM1$^{MATH:NLS}$* was exclusively present in the nucleus (see Supplemental Figure 4B online). Analysis of T4 generation plants showed that the *6xamiBPM* lines consistently had higher WRI1 protein levels comparable to *cul3^{hyp}* mutants, while, surprisingly, all MATH overexpression lines had significantly less WRI1 protein (Figure 3D). Although the absolute degree of WRI1 reduction in MATH overexpression lines varied among tested plants, we never observed any levels that equaled or exceeded those in the wild type. Also of note is that this is not based on reduced *WRI1* expression, since the gene is actually upregulated in *BPM1^{MATH}* and *BPM1$^{MATH:NLS}$* lines (see Supplemental Figure 4C online). Currently, the reasons for this change in WRI1 protein content in the MATH-overexpressing lines remain elusive.

The different plant lines were broadly affected in development. Primary root growth was significantly delayed in all six lines and most strongly in the two *6xamiBPM* lines (Figure 4A). While lateral roots emerged at a lower frequency in the *BPM1^{MATH}* lines, no significant changes were detectable in plants expressing the *BPM1$^{MATH:NLS}$* construct (Figure 4B). The *6xamiBPM* plants developed very low numbers of lateral roots (Figures 4B and 4C), and all transgenic lines were affected in shoot development. In addition, all were late flowering, most strongly pronounced in BPM1^{MATH} and *6xamiBPM* lines (Figures 4D and 4E), with fewer leaves present at the beginning of flowering (Figure 4F) and a reduced rosette size (Figures 4D and 4G). Besides being smaller and present in fewer numbers, the leaves of transgenic plants also had a tendency to develop wider blades than the wild type (see Supplemental Figure 5 online).

To investigate to what extent WRI1 protein stability is affected in the different lines, stability assays were performed on selected plants (Figure 5; see Supplemental Figure 6 online). The assays consistently showed that in either the *6xamiBPM* or MATH-overexpressing backgrounds, WRI1 was highly stable in comparison to the wild type (Figure 5A; see Supplemental Figures 6A and 6B online).

IP experiments were performed on two MATH-overexpressing and two *6xamiBPM* lines. As shown in Figure 5B, CUL3 protein was precipitated from wild-type plant extracts, while no precipitated CUL3 was detectable in either the MATH-overexpressing or

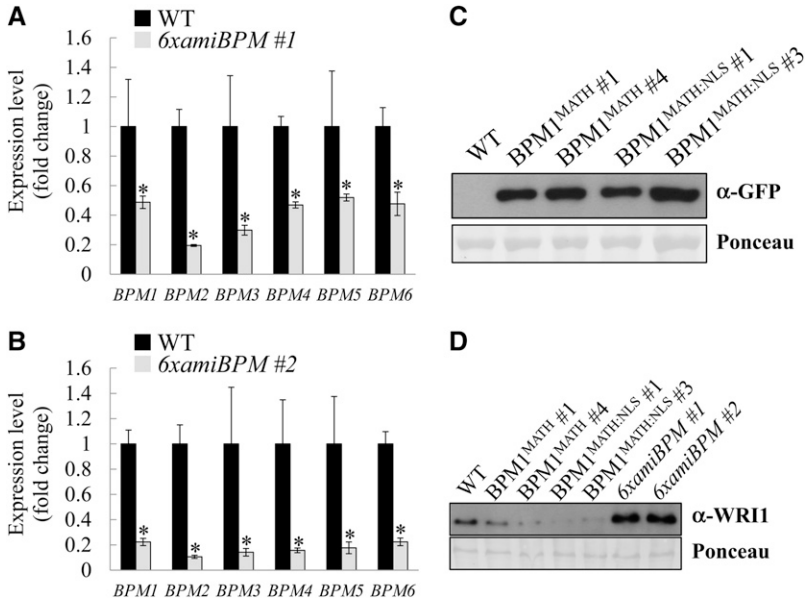

Figure 3. Generation of *6×amiBPM* and MATH-Overexpressing Lines and Their Effect on WRI1 Protein Levels.

(A) and **(B)** qRT-PCR analysis show significantly reduced expression levels for six *BPMs* is in two representative *6×amiBPM* lines compared with the wild type (WT).

(C) Expression levels of BPM1^{MATH} show significant increases in two BPM1^{MATH} lines and two BPM1$^{MATH:NLS}$ lines compared with the wild type.

(D) WRI1 protein content is strongly reduced in MATH-overexpressing lines when compared with the wild type, while both *6xamiBPM* lines display increased WRI1 levels. All asterisks in this and subsequent figures indicate the statistical significant difference of at least $P < 0.05$ (one-way analysis of variance) to the wild type.

6xamiBPM lines. These findings together with stability assays demonstrate that the BPM proteins are required (1) for assembly of WRI1 into a complex with CUL3 and (2) for mediation of the transcription factor's degradation.

WRI1 Activity Is Affected by CRL3^{BPM}

We showed stabilization of WRI1 and an effect on its protein content in the plant in three different genetic backgrounds. In both the *cul3^{hyp}* double mutant and *6xamiBPM* lines, WRI1 levels are higher than the wild type, while in the MATH lines, WRI1 amounts are lower. In *6xamiBPM* lines, *BPM* expression is reduced, and in the *cul3^{hyp}* and MATH backgrounds, BPM protein levels are likely unchanged. However, based on each genetic background, the assembly of WRI1 into a CUL3-based complex is differently affected by either reduced CUL3 availability and/or functionality (*cul3^{hyp}*), reduced BPM content (*6xamiBPM*), or reduced accessibility of BPMs to WRI1 (MATH-overexpressing lines). To investigate whether these situations affect WRI1 transcriptional activities differently, expression of two confirmed WRI1 targets, *BCCP1* and *GLB1*, was tested (Baud et al., 2009; Maeo et al., 2009). *BCCP1* (*At5g16390*), which encodes for a biotin carboxyl carrier protein, and *GLB1* (*At4g01900*), which encodes for a PII protein, are both critical players in fatty acid biosynthesis, but also participate in carbon and nitrogen metabolism (Tissot et al., 1998; Chen et al., 2006).

Quantitative RT-PCR (qRT-PCR) analysis revealed a loss of *BCCP1* and *GLB1* expression in the *wri1-3* null mutant compared with the wild type (Figure 5C). Expression of both genes in MATH-overexpressing lines was similarly reduced. By contrast, both genes were strongly upregulated in *6xamiBPM* lines correlating with changes in WRI1 protein content. Interestingly, no change in *BCCP1* or *GLB1* expression in comparison to the wild type was noticeable in the *cul3^{hyp}* line, despite the fact that WRI1 protein levels were elevated comparable to *6xamiBPM* lines. These findings indicate, based on the presumed presence (*cul3^{hyp}*) or absence (*6xamiBPM*), that BPM proteins also negatively affect transcriptional activity of their target proteins.

CUL3 Assembles with WRI1 at the DNA Level

To investigate whether CUL3 forms a complex with WRI1 at the DNA level, we performed chromatin immunoprecipitation (ChIP) experiments (Morohashi et al. 2009). In wild-type plants, α-WRI1– and α-CUL3–based ChIP experiments resulted in a two- to threefold enrichment of WRI1 binding sites (*proBCCP1* and *proAtGLB1*), respectively (Figure 5D), while no enrichment was detectable in the *wri1-3* null mutant, which served as a negative control (Figure 5G). Interestingly, α-WRI1 ChIP in the two *6xamiBPM* lines yielded higher levels of *proGLB1* and *proBCCP1* sites, which was in agreement with higher WRI1 protein levels in these plants (Figures 5E and 5F), as well as increased transcription of the corresponding genes (Figure 5C). Finally, ChIP using the α-CUL3 antibody in *6xamiBPM* lines did not lead to any enrichment of *proGLB1* and *proBCCP1* sites (Figures 5E and 5F), which corroborates the finding that loss of BPMs disrupt the

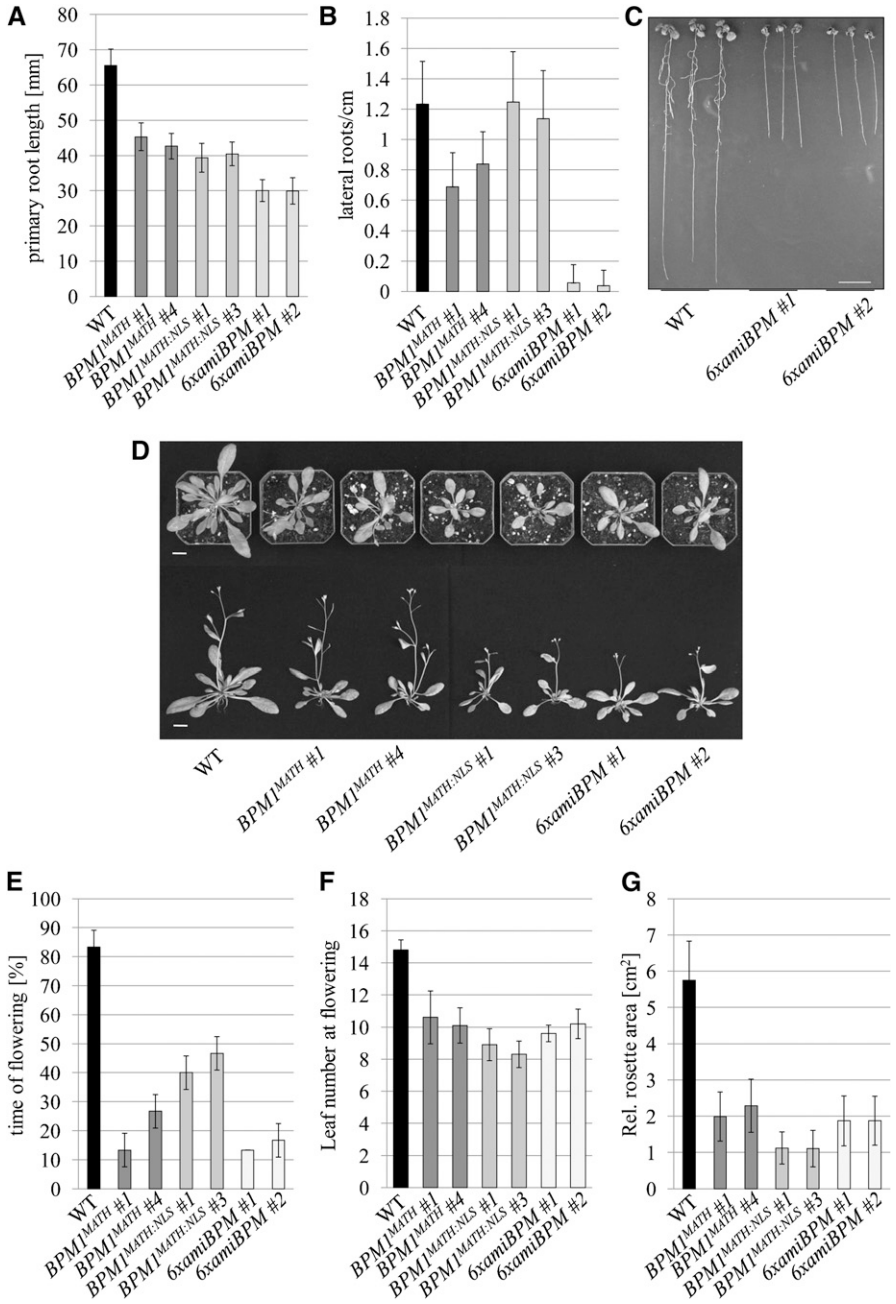

Figure 4. Phenotype Analysis of the Wild Type, Two *6×amiBPM* Lines, and MATH-Overexpressing Lines.

(A) Primary root lengths of 2-week-old *Arabidopsis* seedlings are strongly reduced in all transgenic lines when compared with the wild type (WT; *n* = 45).
(B) Specifically, *6xamiBPM* plants have reduced numbers of lateral roots development (2-week-old seedlings; *n* = 45).
(C) Root phenotype of wild-type and two *6×amiBPM* lines. Picture was taken 14 d after germination.
(D) Overview of rosette phenotypes from wild-type and transgenic lines. Picture was taken 33 d after germination.
(E) All transgenic lines are late flowering. Data were taken for 33-d-old plants (*n* = 30).
(F) Rosette leaf number at time of flowering (*n* = 10).
(G) Rosette area of 25-d-old *Arabidopsis* plants for each genetic background (*n* = 30).

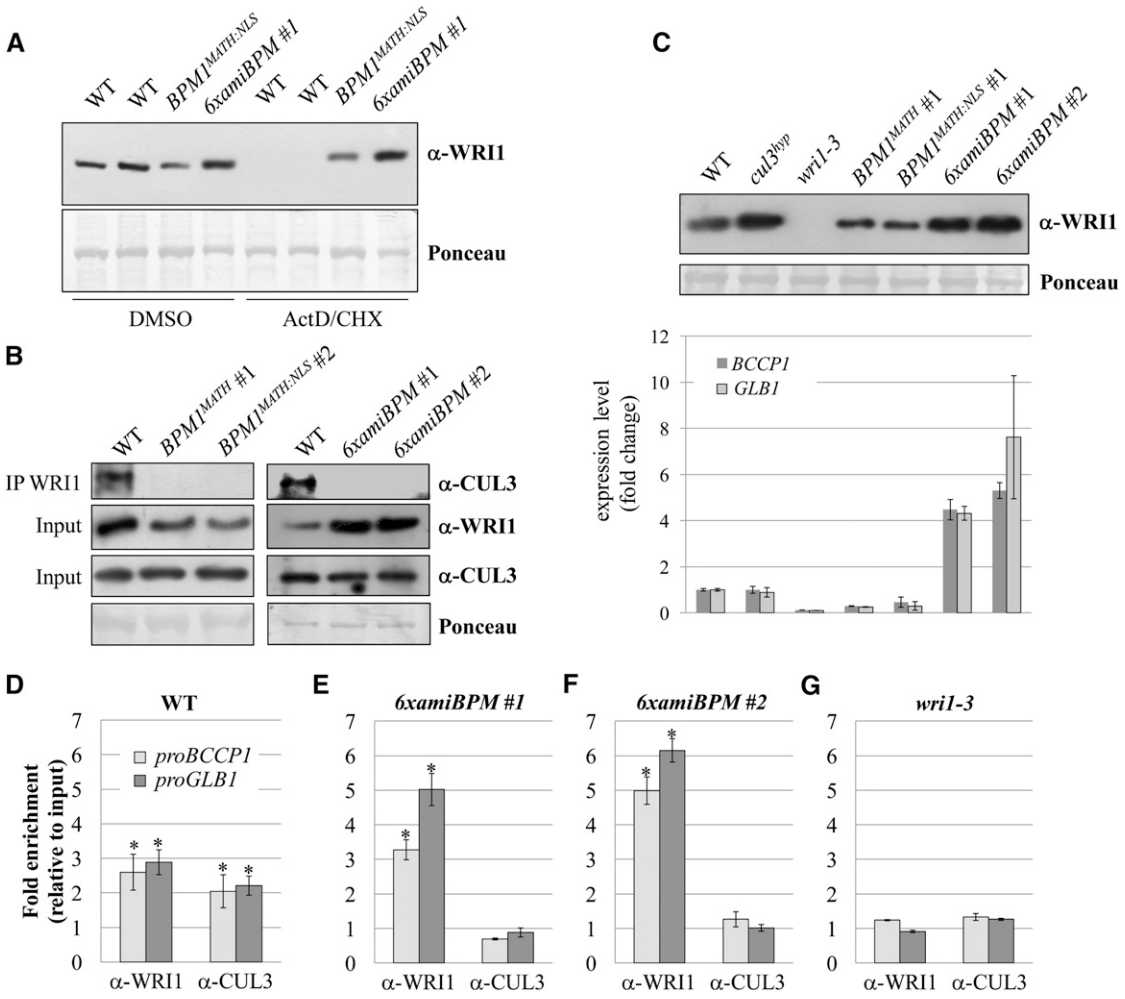

Figure 5. Studies of WRI1's Protein Level, WRI1's Transcriptional Activity, and Complex Assembly at the DNA Level.

(A) WRI1 protein is stabilized in MATH overexpressing and *6×amiBPM* lines. WT, the wild type.
(B) CUL3 could be precipitated with α-WRI1 from wild-type plant extracts but not from BPM1^{MATH} (left half) or *6×amiBPM* (right half) extracts. Input was tested for presence of WRI1 and CUL3 proteins using the respective antibodies.
(C) Protein levels of WRI1 and expression of two WRI1 target genes, *GLB1* and *BCCP1*, in the wild type and the different transgenic backgrounds.
(D) to **(G)** ChIP–quantitative PCR analysis on the wild type, two *6xamiBPM* lines, and *wri1-3* shows enrichment of the two WRI1 target promoters *proBCCP1* and *proGLB1* in the wild type **(D)** but not in a *wri1-3* mutant **(G)** after IP with either α-WRI1 or α-CUL3 antibodies. While no enrichment was detectable in samples derived from α-CUL3 ChIPs in two *6xamiBPM* lines (**[E]** and **[F]**), significant enrichment was detectable in α-WRI1 ChIP samples when compared with the wild type (**[E]** and **[F]**). ChIP–quantitative PCR experiments were repeated at least three times independently. Error bar indicates the SE. Asterisk indicates a statistical significant difference (one-way analysis of variance, $P < 0.05$) compared with individual control.

ability of CUL3 to assemble into a complex with WRI1 (Figure 5B). Overall, these results provide strong evidence that CUL3 proteins form a complex with WRI1 at the DNA level and that this assembly requires BPM proteins.

Reduced BPM Content Affects Fatty Acid Metabolism in Seeds

The finding that reduced *BPM* expression in *6xamiBPM* lines increases both WRI1 protein content and expression of WRI1 target genes was intriguing as it opened up the possibility that seeds of *6xamiBPM* lines may also contain elevated levels of fatty acids due to augmented levels of active WRI1 (Baud et al., 2009). In agreement with this idea, both *6xamiBPM* lines showed significant increases in seed weights and size when compared with wild-type seeds (Figures 6A and 6B). However, changes were much more pronounced in *6xamiBPM #1* than in *6xamiBPM #2* plants, which may be due to different activities of the 35S promoter in seeds of the two lines. The lines also showed increased WRI1 content in seeds and elevated expression of the two target genes *BCCP1* and *GLB1* (Figure 6C). Similar to their increases in weight, both lines also showed altered total fatty acid contents (Figure 6D); while changes in *6xamiBPM #2* plants were only very mild and furthermore nonsignificant (~96 μg/30 seeds in average

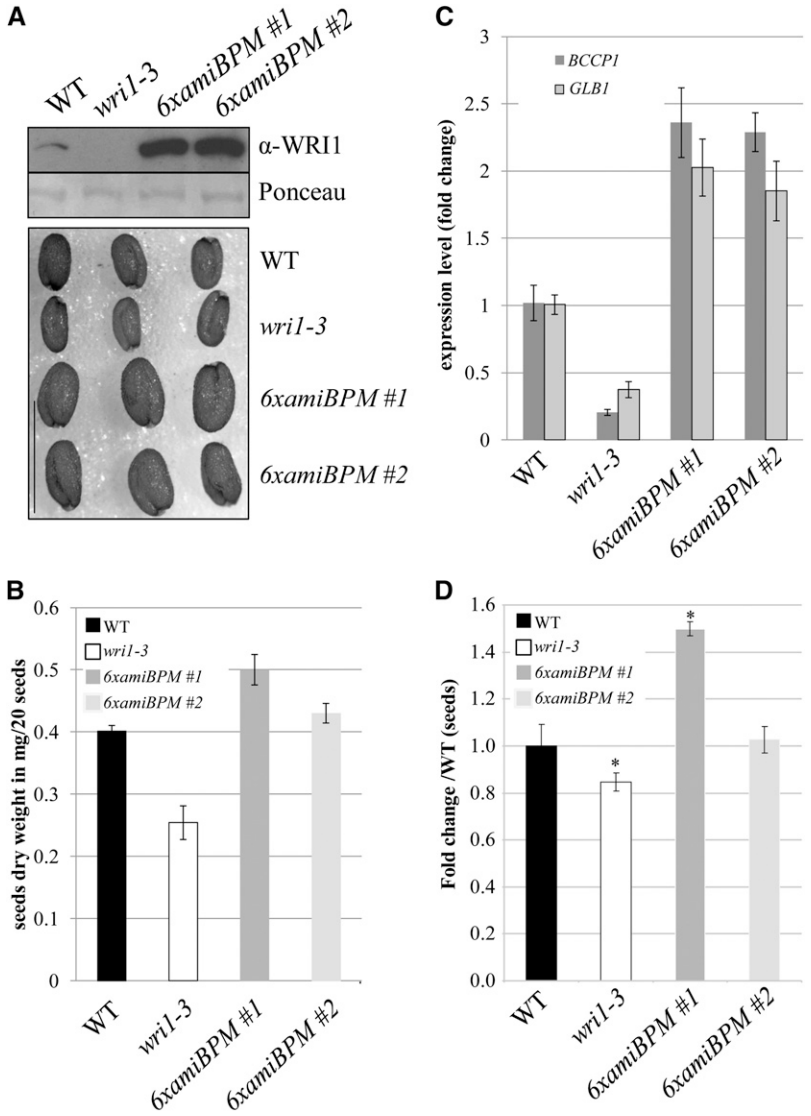

Figure 6. Seed Weight, Size, and Fatty Acid Content in Wild-Type, *wri1-3*, and *6xamiBPM* Plants.

(A) and **(B)** In comparison to the wild type (WT), seed weight and size is significantly reduced in *wri1-3*, while it is increased in both *6xamiBPM* lines and to a greater extend in *6xamiBPM#1* then it is in *#2*. Bar in **(A)** = 1 mm. Data in **(B)** represent average of $n = 5$ measurements of 20 seeds.
(C) Seeds in *6xamiBPM* lines contain higher WRI1 levels, which correlate with expression of the WRI1 target genes *BCCP1* and *GLB1*.
(D) Fold change in fatty acid contents of *wri1-3* and the two *6xamiBPM* lines in comparison to the wild type. Data represent average of $n = 5$ measurements of 30 seeds. The asterisk shows a statistically significant difference compared with the wild type ($P < 0.05$, *t* test).

versus ~93 μg/30 seeds in the wild type), the total fatty acid content in *6xamiBPM #1* seeds was increased by around 50% (~140 μg/30 seeds) when compared with the wild type. The *wri1-3* line was used in these experiments as a control and showed a significant reduction in both seed weight and total fatty acid contents (~79 μg/30 seeds) when compared with the wild type and the two *6xamiBPM* lines. While changes were observable for total fatty acid content, measurements of individual fatty acids did not detect any significant changes (see Supplemental Figure 7 online). In addition, no significant changes were observed in a general metabolic profile (amino and organic acids as well as soluble sugar) for *wri1-3* or the two *amiBPM* lines when compared with the wild type (see Supplemental Figure 7 online), indicating that the changes in seed size and weight for the mutants are primarily based on aberrant fatty acid contents. Overall, these data further underscore that BPM proteins are critical regulators of WRI1 activity and that their loss positively affects both WRI1 stability as well as its actions.

Because seeds of the two *6xamiBPM* lines varied significantly in their weight and fatty acid content, we included a third *6xamiBPM* line in our analysis to ensure that loss of BPMs leads to increases in fatty acid content and seed size in a reproducible manner. As

observed for the other two lines, *6xamiBPM #3* seeds are also increased in size (see Supplemental Figure 8B online) as well as in dry weight (see Supplemental Figure 8C online), and this correlated with elevated WRI1 content (see Supplemental Figure 8A online), as well as upregulated expression of *BCCP1* and *GLB1* (see Supplemental Figure 8D online). Likewise, we also observed a significant increase in fatty acid content in these seeds in comparison to the wild type (see Supplemental Figure 8E online), substantiating the finding for *6xamiBPM #1* plants that reduced BPM activity likely results in higher fatty acid levels in seeds.

DISCUSSION

This work shows that BPM proteins have the ability to interact with a broad range of ERF/AP2 proteins. Although in planta assembly has only been confirmed for WRI1, Y2H studies still strongly indicate that many ERF/AP2 proteins are targeted in *Arabidopsis* by a CRL3^{BPM} complex. IP and pull-down studies in this work underscore that WRI1 assembles in vitro and in the plant into a complex with CUL3, and the missing CUL3-WRI1 assembly in *6xamiBPM* and MATH-overexpressing backgrounds emphasizes that BPM proteins are required for this step. The studies further show that the interaction of BPMs with WRI1 results in the destabilization of their substrate. This is supported by the finding that WRI1 is stabilized in a *cul3^{hyp}* background, as well as in MATH overexpression and *6xamiBPM* plants. Moreover, the ChIP data strongly support our assumption that WRI1-CRL3^{BPM} assembly occurs at the DNA level. Consequently, BPM proteins can be considered as negative regulators of WRI1 activities by mediating assembly with the CRL3 core and ultimately causing its degradation via the 26S proteasome. This is also supported by the finding that fatty acid levels are significantly increased in seeds of *6xamiBPM #1* and #3 plants. These changes resemble earlier descriptions for plants overexpressing WRI1 (Cernac and Benning, 2004). However, it is significant to note that similar changes can be accomplished in *Arabidopsis* without ectopically expressing a transgenic WRI1 in seeds. The fact that overall metabolic changes were mostly restricted to total fatty acid contents also indicates that the function of BPM proteins in seeds is strongly connected with WRI1 activity. In this context, it is of note that WRI1 has very recently been described as part of a small gene family with a total of four members in *Arabidopsis* (To et al., 2012). Although WRI1 is the primary member that regulates fatty acid biosynthesis in seeds, the other members also contribute to this pathway, but they do so in other tissues (To et al., 2012). Consequently, it will be interesting to see whether these other WRI1-related proteins also underlie the control of CRL3^{BPM} E3 ligase activities. Our findings also support the earlier suggestion that instability of RAP2.4, another BPM interacting protein, is mediated by a CRL3^{BPM} ligase (Weber and Hellmann, 2009). Overall, it is likely that a general consequence of BPM interaction with ERF/AP2 transcription factors is degradation of the latter.

In this context, it is also important to note that the BPM family members have very recently been established as regulators of an ABA response by targeting the homeodomain Leucine zipper transcription factor HB6 for degradation (Lechner et al., 2011). Consequently, plants with reduced levels of *BPM1*, *4*, *5*, and *6* (*amiR-bpm*) display aberrant responses in stomatal opening (Lechner et al., 2011); however, germinating *amiR-bpm* seedlings only display increased ABA resistance when combined with an *HB6* overexpression background. The finding that a member of another transcription factor family is a substrate of BPM proteins further increases the number of potential substrate proteins that are targeted by CRL3^{BPM} for degradation. Furthermore, many members of the ERF/AP2 family have been described in context with stress tolerance, including the ones tested in this study. For example, DREB1a is a classical regulator of drought and cold tolerance responses in plants (Sakuma et al., 2002; Miura et al., 2007). ERF1 is known to play a role in biotic stress (Lorenzo et al., 2003; Zhang et al., 2011), and RAV1 has been described in context with senescence and different abiotic stress conditions (Sohn et al., 2006; Woo et al., 2010; Yun et al., 2010). It is therefore likely that both MATH overexpression and *6xamiBPM* plants display different sensitivities toward stress, such as cold or drought, as well as treatments with phytohormones, such as ethylene or jasmonic acid, in addition to ABA.

It is also noteworthy that degradation of WRI1 appears to occur continuously rather than being stimulated by a specific signal, and this also holds true for RAP2.4 and HB6 (Weber and Hellmann, 2009; Lechner et al., 2011). It is unlikely that the cell is always degrading these proteins to the same amount since this seems to be quite an inefficient and uneconomical approach to regulating protein amounts. Rather, one would expect that specific signals are in place that slow down turnover of CRL3^{BPM} substrates in a similar manner to the process that occurs in ethylene signal transduction, where ethylene disrupts proteasomal degradation of EIN3 mediated by the F-box proteins EBF1 and EBF2 (Guo and Ecker, 2003; Potuschak et al., 2003). In fact, ABA treatment appears to have a stabilizing effect on HB6, but the kind of signal that may have a similar effect on WRI1 or RAP2.4 remains unclear.

The wide-ranging developmental changes in both *6xamiBPM*, as well as MATH overexpression lines, emphasizes that the BPM family is widely required for plant development. *amiR-BPM* plants showed reduced shoot growth (Lechner et al., 2011), which we also observed for *6xamiBPM* lines. Interestingly, we could not detect any problems in fertility as observed by Lechner et al. (2011) for *amiR-bpm* plants. This opens up the question of whether BPM3 and 4, which are not affected in *amiR-bpm* lines, may have specific roles in flower development. In addition, *6xamiBPM* plants had strongly reduced root development and fewer leaves, and it remains open whether these changes were also seen by Lechner et al. (2011). Moreover, changes in root development were not apparent in MATH overexpression lines, indicating that reduced *BPM* expression and binding competition approaches affected the developmental program of the roots in the corresponding plants differently.

The different approaches employed in this work to affect the CRL3^{BPM}-WRI1 interplay revealed two additional interesting aspects about the function of BPM proteins besides being substrate receptors to a CRL3^{BPM} ligase. First, comparing *cul3^{hyp}* and *6xamiBPM* plants clearly demonstrated that in both genetic backgrounds, WRI1 protein content is increased due to greater stability of the transcription factor. However, the transcriptional activity of WRI1 was only elevated in *6xamiBPM* plants but not in *cul3^{hyp}*, as indicated by the changed versus unchanged

transcriptional levels of *GLB1* and *BCCP1*. Given that in the *cul3*^{hyp} mutant, BPM protein levels are likely normal, these findings indicate that BPM proteins negatively interfere with WRI1 activity, most likely by binding to the transcription factor, while more active WRI1 is available in *6xamiBPM* plants. Second, the reduced WRI1 amount was quite surprising and unexpected. Because *WRI1* expression was upregulated in MATH overexpressors, one may suggest that the reduced WRI1 content was sensed by the cell and that changes on the transcriptional level represent a feedback-loop response. In addition, these data also clearly indicate that the MATH domain also interfered with posttranscriptional processes and thus point out that BPM proteins may have even further diverse roles in addition to targeting ERF/AP2 or HB6 transcription factors for ubiquitylation and proteasomal degradation.

Finally, it is of interest that the ChIP data strongly indicate that the CRL3^{BPM} E3 ligase assembles with WRI1 at the DNA level, while the transcription factor is bound to its target sites. At this point, we cannot judge whether the CRL3^{BPM} complex only assembles with WRI1, and potentially other substrates, exclusively at the DNA level or whether this also occurs independently of DNA binding. In addition, it is also undetermined whether BPMs assemble independently of CUL3 with their substrates. These open questions need to be addressed in future work.

In summary, this work reveals a link between fatty acid metabolism and CUL3-based E3 ligase activities. The work also confirms that BPM proteins function in planta as substrate receptor proteins to a CRL3^{BPM} ligase with the purpose of destabilizing bound substrates. These findings further indicate that a large number of ERF/AP2 proteins are potential targets of BPM proteins and that this complex plays a major role in plant development and stress tolerance by broadly regulating transcriptional, and potentially posttranscriptional, processes in the plant.

METHODS

Plant Materials and Growth Conditions

Arabidopsis thaliana wild-type ecotype Columbia plants and plants of the different genetic backgrounds were grown either on *Arabidopsis thaliana* (AT) medium without supplement of Suc (Estelle and Somerville, 1987) in a growth chamber at 22°C with 120 μmol/m^2/s light intensity or in soil in a greenhouse at 20°C under long-day conditions (16 h light/8 h dark).

Clone Constructions

The cDNAs of *BPM1*^{MATH}, *BPM1*$^{MATH:NLS}$, *CUL3s*, *ERF/AP2s*, and *BPMs* were cloned into *pDONR221* (Invitrogen). For Y2H studies, the corresponding cDNAs were shuffled into destination vectors *pACT2* (prey) and *pBTM116-D9* (bait) by Gateway technology (Invitrogen) as described (Weber et al., 2005). *pDEST15* (Invitrogen) and *pET-58-DEST* (Merck) were used to express and purify GST- and His-tagged proteins in *Escherichia coli*, respectively; where necessary, elution of GST proteins from glutathione-agarose beads was done following standard procedures. *pMDC43* was used for expression in plants and for subcellular localization studies as described (Curtis and Grossniklaus, 2003). The NLS sequence was adopted from Howard et al. (1992), extended, and attached to the *MATH* domain in a four-step-based PCR process. To generate artificial microRNAs, a protocol from the WMD2 microRNA designer Web page (http://wmd2.weigelworld.org; see Supplemental Figure 9 online) was followed using *pRS300* as starting vector. For expression in plants, *ami* constructs were first cloned into *pDONR221* before being shuffled into the binary vector *pGBW14*. For primers used, see Supplemental Table 1 online.

Subcellular Localization Studies

The fluorescent fusion proteins GFP:WRI1, GFP:BPM1^{MATH}, and BPM1$^{MATH:NLS}$ were transiently expressed in *Nicotiana benthamiana* epidermal cells following the method described by Sparkes et al. (2006). GFP expression was detected and documented with a Zeiss LSM 510 Meta confocal microscope.

Interaction and Complex Assembly Studies

Y2H studies were followed as described by Weber et al. (2005). SDII selection medium supplemented with uracil and His was used as transformation control, while for interaction studies, SDIV minimal medium was chosen without uracil and His supplements. Photos were taken from single spots 7 d after plating. FPLC was performed with 2 mg protein injections and a flow rate of 50 μL/min using an AKTA FPLC system (GE Healthcare Science) and as described by Leuendorf et al. (2010). Pull-down analysis and IP studies were followed as described before (Hellmann et al., 2003; Bernhardt et al., 2006). Extraction and washing buffers contained at all times 1 mM PMSF (Sigma-Aldrich) and 10 μM MG132 (Sigma-Aldrich) to prevent proteolytic and proteasomal activities, respectively. For pull-down analysis with GST- and His-tagged proteins, GST-containing proteins were first eluted from glutathione-agarose beads before incubated with His:WRI1 that remained attached to tetradentated-chelated nickel resin. In general, proteins were incubated at least 1.5 h at 4°C under shaking conditions before being centrifuged. Precipitates were washed no less than three times to remove unspecific bindings, before they were taken up in Laemmli buffer (Laemmli, 1970) and boiled (10 min, 95°C). IPs were followed as described by Bernhardt et al. (2006). In brief, 1 mg of fresh protein extracts from 2-week-old seedlings were precleaned with 30 μL protein-A-agarose beads (Santa Cruz Biotechnology; 1.5 h, 4°C). The beads were centrifuged, and the supernatant was transferred into a fresh tube and incubated first with α-WRI1 (1.5 h, 4°C) before 30 μL protein-A-agarose beads were added (1.5 h, 4°C). After brief centrifugation, four washing steps followed, after which precipitates were taken up in Laemmli buffer and boiled as described above. For pull-down and IP studies, precipitates were further analyzed by SDS-PAGE and protein gel blotting using standard procedures. Where applicable, membranes were stained with Ponceau S to detect transferred proteins. For immunodetection, custom-made (α-CUL3 [rabbit] and α-WRI1 [rabbit]; GeneScript) or commercially available antibodies (GST, secondary α-rabbit IgG-horseradish peroxidase; Santa Cruz) in combination with an ECL Plus Western Blotting Detection Kit (GE Healthcare Life Science) were used.

Stability Assays

For stability assays, *Arabidopsis* seedlings were cultured on solid AT medium for 2 weeks before being transferred to 5 mL AT liquid medium. Plants were incubated for 3 h with the transcriptional inhibitor ActD2 (Sigma-Aldrich; final concentration 10 μg/mL) and/or the proteasomal inhibitor MG132 (Sigma-Aldrich; 20 μM/mL, 6 h) before CHX (Sigma-Aldrich; 100 μM/mL, 3 h) was added to inhibit translation. DMSO was used as mock control and as a dissolvent for all inhibitors. Protein gel blot analysis and protein detection were conducted using standard procedures. The antibodies against WRI1 and CUL3 were designed and produced by GeneScript and used in a 1:1000 dilution. Protein detection was followed as described in the ECL Plus Western Blotting Detection Kit manual (GE Healthcare Life Science).

RNA Isolation and Expression Analysis

Total *Arabidopsis* RNA was extracted following the protocol of the Isolate RNA kit from Bioline; reverse transcription was done according to the manual for the high-capacity cDNA reverse transcription kit (Applied Biosystems). qRT-PCR reactions (95°C, 7 min; 95°C, 15 s; 60°C, 1 min; 40 cycles) were performed using the SYBR green method on a 7500 Fast Real-Time PCR system (Applied Biosystems). Relative gene expression analyses were calculated by the full quantification method with *ACTIN2* as the internal control gene. Fourteen 2-week-old seedlings were pooled for each replicate. At least three biological replicates were performed for each individual experiment. Primers used for qRT-PCR are shown in Supplemental Table 1 online.

ChIP Assays

For ChIP assays, an established protocol was followed (Morohashi et al., 2009). In brief, 60 mg (fresh weight) of 15-d-old seedlings were harvested for each ChIP experiment and cross-linked for 10 min under vacuum in cross-link buffer containing 1% formaldehyde as described by Morohashi et al. (2009). Cross-linked samples were incubated in 100 mM Gly for 5 min under a vacuum, thoroughly washed in double-distilled water, and snap frozen in liquid nitrogen. Frozen tissues were ground into fine powder and dissolved in nuclear isolation buffer (Morohashi et al., 2009) supplemented with 1× protease inhibitor cocktail (Sigma-Aldrich). After filtering through single-layered Miracloth (Merck), the samples were centrifuged (10 min, 1200*g*, 4°C). Pellets were resuspended in nuclear isolation buffer supplemented with 0.3% Triton X-100 and centrifuged again (10 min, 10,000*g*, 4°C). After resuspension in lysis buffer, the purified nuclei were then sonicated (three times, 20 s, 9 W; Fisher Scientific Model 100 dismembrator) to yield chromatin fragments of 300 to 500 bps. Sonicated chromatin fragments (2 mg) were first precleared with protein-A-agarose beads (Sigma-Aldrich) (1.5 h, 4°C) before being incubated with specific antibodies (1 mg/mL; 1.5 h, 4°C), followed by a fresh batch of protein-A-agarose beads (30 μL; 1.5 h, 4°C) to IP protein-DNA complexes. After IP, cross-linking was reversed by incubating samples overnight at 65°C in elution buffer (1% SDS, 0.1 M $NaHCO_3$, and 0.25 mg/mL proteinase K; Morohashi et al., 2009), after which RNaseA (1 mg/mL) was added (30 min; room temperature). As input control for data normalization, a portion of sonicated, cross-linked, and precleared DNA was treated accordingly except for undergoing an IP. Samples were further cleaned up using a DNA purification kit (NuCleoSpin Extraction II; Macherey-Nagel) and quantified to use equal amounts of template (50 ng/reaction) for qRT-PCR analysis. To amplify promoter sequences that contain an AW-box recognized by WRI1 (Maeo et al., 2009), specific primers were designed (see Supplemental Table 1 online). EF1 was selected as a reference gene for internal control. qRT-PCR reactions (95°C, 10 min; 95°C, 15 s; 60°C, 1 min; 50 cycles) were done as described above and repeated with at least three independent biological replicates.

Metabolic Analysis

Metabolic profiling of 2-week-old seedlings grown on ATS plate (100 mg fresh weight) and seed samples (50 mg dry weight) of all backgrounds used in this study were analyzed according to earlier described protocols (Roessner-Tunali et al., 2003). Seed fatty acids were extracted exactly as described before (Focks and Benning, 1998). For quantification with gas chromatography, pentadecanoic acid was used as an internal standard (Browse et al., 1985).

Accession Numbers

Sequence data from this article can be found in the GenBank/EMBL data libraries under the following accession numbers: ACTIN2, At3g18780; IAA5, At1g15580; BPM1, At5g19000; BPM2, At3g06190; BPM3, At2g39760; BPM4, At3g03740; BPM5, At5g21010; BPM6, At3g43700; DREB1a, At4g25480; ERF1, At3g23240; ERF4, At3g15210; RAV1, At1g13260; WRI1, At3g54320; BCCP1, At5g16390; and GLB1, At2g16060.

Supplemental Data

The following materials are available in the online version of this article.

Supplemental Figure 1. Verification of α-CUL3 and α-WRI1 Antibodies.

Supplemental Figure 2. FPLC Analysis and Subcellular Localization of WRI1.

Supplemental Figure 3. CHX Treatment Does Not Reduce the Protein Level of WRI1, but It Induces Its Transcription Level.

Supplemental Figure 4. Subcellular Localization of GFP:BPM1^{MATH} and GFP:BPM1$^{MATH:NLS}$.

Supplemental Figure 5. Rosette Leaf Phenotype on the Time of Primary Inflorescence.

Supplemental Figure 6. Stability Assays of WRI1 in Wild-Type, *6×amiBPM*, and MATH Overexpressing Lines.

Supplemental Figure 7. Fatty Acid Profile and Metabolic Profile in Seeds of Wild-Type, *wri1-3*, and Two *6xamiBPM* Lines.

Supplemental Figure 8. Seed Phenotype Analyses for *6xamiBPM #3*.

Supplemental Figure 9. Predicted Target Sites for Artificial MicroRNA (in Red) on the Different *BPM* Genes.

Supplemental Table 1. Primers Used for Different PCR-Based Approaches.

ACKNOWLEDGMENTS

We thank Sutton Mooney for technical support and critical reading, the National Science Foundation for support to H.H. (MCB-1020673) and S. R. (MCB-1052492), Detlef Weigel for providing the vector *pRS300*, and Pascal Genschik for seeds of *cul3^{hyp}*. We also thank Kengo Morohashi and Erich Grotewold for technical advice on ChIP.

AUTHOR CONTRIBUTIONS

H.W. originally found WRI1 and ERF4 as interactors of BPM proteins through Y2H and pull-down studies. J.H.L. generated the *6×amiBPM* and MATH-overexpressing lines and generated confocal microscopy pictures. L.C. contributed to clone constructions, Y2H studies, complex assembly analysis, ChIP, stability assays, RNA isolation, expression analysis, and *Arabidopsis* phenotypical analyses. S.R. helped with the FPLC experiments. T.T., S.W., and A.R.F. provided the metabolic data. H.H. is the principal investigator for this National Science Foundation–supported project; he participated in complex assembly analysis and in writing the article.

Received November 9, 2012; revised May 22, 2013; accepted June 3, 2013; published June 21, 2013.

REFERENCES

Baud, S., Wuillème, S., To, A., Rochat, C., and Lepiniec, L. (2009). Role of WRINKLED1 in the transcriptional regulation of glycolytic and fatty acid biosynthetic genes in *Arabidopsis*. Plant J. **60:** 933–947.

Bernhardt, A., Lechner, E., Hano, P., Schade, V., Dieterle, M., Anders, M., Dubin, M.J., Benvenuto, G., Bowler, C., Genschik, P., and Hellmann, H. (2006). CUL4 associates with DDB1 and DET1

and its downregulation affects diverse aspects of development in *Arabidopsis thaliana*. Plant J. **47:** 591–603.

Browse, J., McCourt, P., and Somerville, C.R. (1985). A mutant of *Arabidopsis* lacking a chloroplast-specific lipid. Science **227:** 763–765.

Cernac, A., and Benning, C. (2004). WRINKLED1 encodes an AP2/EREB domain protein involved in the control of storage compound biosynthesis in *Arabidopsis*. Plant J. **40:** 575–585.

Chen, Y.M., Ferrar, T.S., Lohmeier-Vogel, E.M., Morrice, N., Mizuno, Y., Berenger, B., Ng, K.K., Muench, D.G., and Moorhead, G.B. (2006). The PII signal transduction protein of *Arabidopsis thaliana* forms an arginine-regulated complex with plastid N-acetyl glutamate kinase. J. Biol. Chem. **281:** 5726–5733. Erratum. J. Biol. Chem. **281:** 24084.

Curtis, M.D., and Grossniklaus, U. (2003). A gateway cloning vector set for high-throughput functional analysis of genes in planta. Plant Physiol. **133:** 462–469.

Dieterle, M., Thomann, A., Renou, J.P., Parmentier, Y., Cognat, V., Lemonnier, G., Müller, R., Shen, W.H., Kretsch, T., and Genschik, P. (2005). Molecular and functional characterization of *Arabidopsis* Cullin 3A. Plant J. **41:** 386–399.

Estelle, M.A., and Somerville, C. (1987). Auxin resistant mutants of *Arabidopsis thaliana* with altered morphology. Mol. Gen. Genet. **206:** 200–206.

Figueroa, P., Gusmaroli, G., Serino, G., Habashi, J., Ma, L., Shen, Y., Feng, S., Bostick, M., Callis, J., Hellmann, H., and Deng, X.W. (2005). *Arabidopsis* has two redundant Cullin3 proteins that are essential for embryo development and that interact with RBX1 and BTB proteins to form multisubunit E3 ubiquitin ligase complexes in vivo. Plant Cell **17:** 1180–1195.

Focks, N., and Benning, C. (1998). *wrinkled1*: A novel, low-seed-oil mutant of *Arabidopsis* with a deficiency in the seed-specific regulation of carbohydrate metabolism. Plant Physiol. **118:** 91–101.

Gingerich, D.J., Gagne, J.M., Salter, D.W., Hellmann, H., Estelle, M., Ma, L., and Vierstra, R.D. (2005). Cullins 3a and 3b assemble with members of the broad complex/tramtrack/bric-a-brac (BTB) protein family to form essential ubiquitin-protein ligases (E3s) in *Arabidopsis*. J. Biol. Chem. **280:** 18810–18821.

Gingerich, D.J., Hanada, K., Shiu, S.H., and Vierstra, R.D. (2007). Large-scale, lineage-specific expansion of a bric-a-brac/tramtrack/broad complex ubiquitin-ligase gene family in rice. Plant Cell **19:** 2329–2348.

Guo, H., and Ecker, J.R. (2003). Plant responses to ethylene gas are mediated by SCF(EBF1/EBF2)-dependent proteolysis of EIN3 transcription factor. Cell **115:** 667–677.

Hellmann, H., Hobbie, L., Chapman, A., Dharmasiri, S., Dharmasiri, N., del Pozo, C., Reinhardt, D., and Estelle, M. (2003). *Arabidopsis* AXR6 encodes CUL1 implicating SCF E3 ligases in auxin regulation of embryogenesis. EMBO J. **22:** 3314–3325.

Howard, E.A., Zupan, J.R., Citovsky, V., and Zambryski, P.C. (1992). The VirD2 protein of *A. tumefaciens* contains a C-terminal bipartite nuclear localization signal: Implications for nuclear uptake of DNA in plant cells. Cell **68:** 109–118.

Hua, Z., and Vierstra, R.D. (2011). The cullin-RING ubiquitin-protein ligases. Annu. Rev. Plant Biol. **62:** 299–334.

Laemmli, U.K. (1970). Cleavage of structural proteins during the assembly of the head of bacteriophage T4. Nature **227:** 680–685.

Lechner, E., Leonhardt, N., Eisler, H., Parmentier, Y., Alioua, M., Jacquet, H., Leung, J., and Genschik, P. (2011). MATH/BTB CRL3 receptors target the homeodomain-leucine zipper ATHB6 to modulate abscisic acid signaling. Dev. Cell **21:** 1116–1128.

Leuendorf, J.E., Osorio, S., Szewczyk, A., Fernie, A.R., and Hellmann, H. (2010). Complex assembly and metabolic profiling of *Arabidopsis thaliana* plants overexpressing vitamin B_6 biosynthesis proteins. Mol. Plant **3:** 890–903.

Lorenzo, O., Piqueras, R., Sánchez-Serrano, J.J., and Solano, R. (2003). ETHYLENE RESPONSE FACTOR1 integrates signals from ethylene and jasmonate pathways in plant defense. Plant Cell **15:** 165–178.

Maeo, K., Tokuda, T., Ayame, A., Mitsui, N., Kawai, T., Tsukagoshi, H., Ishiguro, S., and Nakamura, K. (2009). An AP2-type transcription factor, WRINKLED1, of *Arabidopsis thaliana* binds to the AW-box sequence conserved among proximal upstream regions of genes involved in fatty acid synthesis. Plant J. **60:** 476–487.

Miura, K., Jin, J.B., Lee, J., Yoo, C.Y., Stirm, V., Miura, T., Ashworth, E.N., Bressan, R.A., Yun, D.J., and Hasegawa, P.M. (2007). SIZ1-mediated sumoylation of ICE1 controls CBF3/DREB1A expression and freezing tolerance in *Arabidopsis*. Plant Cell **19:** 1403–1414.

Morohashi, K., Xie, Z., and Grotewold, E. (2009). Gene-specific and genome-wide ChIP approaches to study plant transcriptional networks. Methods Mol. Biol. **553:** 3–12.

Potuschak, T., Lechner, E., Parmentier, Y., Yanagisawa, S., Grava, S., Koncz, C., and Genschik, P. (2003). EIN3-dependent regulation of plant ethylene hormone signaling by two *Arabidopsis* F box proteins: EBF1 and EBF2. Cell **115:** 679–689.

Roessner-Tunali, U., Urbanczyk-Wochniak, E., Czechowski, T., Kolbe, A., Willmitzer, L., and Fernie, A.R. (2003). De novo amino acid biosynthesis in potato tubers is regulated by sucrose levels. Plant Physiol. **133:** 683–692.

Sakuma, Y., Liu, Q., Dubouzet, J.G., Abe, H., Shinozaki, K., and Yamaguchi-Shinozaki, K. (2002). DNA-binding specificity of the ERF/AP2 domain of *Arabidopsis* DREBs, transcription factors involved in dehydration- and cold-inducible gene expression. Biochem. Biophys. Res. Commun. **290:** 998–1009.

Sohn, K.H., Lee, S.C., Jung, H.W., Hong, J.K., and Hwang, B.K. (2006). Expression and functional roles of the pepper pathogen-induced transcription factor RAV1 in bacterial disease resistance, and drought and salt stress tolerance. Plant Mol. Biol. **61:** 897–915.

Sparkes, I.A., Runions, J., Kearns, A., and Hawes, C. (2006). Rapid, transient expression of fluorescent fusion proteins in tobacco plants and generation of stably transformed plants. Nat. Protoc. **1:** 2019–2025.

Thomann, A., Lechner, E., Hansen, M., Dumbliauskas, E., Parmentier, Y., Kieber, J., Scheres, B., and Genschik, P. (2009). *Arabidopsis* CULLIN3 genes regulate primary root growth and patterning by ethylene-dependent and -independent mechanisms. PLoS Genet. **5:** e1000328.

Tissot, G., Pepin, R., Job, D., Douce, R., and Alban, C. (1998). Purification and properties of the chloroplastic form of biotin holocarboxylase synthetase from *Arabidopsis thaliana* overexpressed in *Escherichia coli*. Eur. J. Biochem. **258:** 586–596.

To, A., Joubès, J., Barthole, G., Lécureuil, A., Scagnelli, A., Jasinski, S., Lepiniec, L., and Baud, S. (2012). WRINKLED transcription factors orchestrate tissue-specific regulation of fatty acid biosynthesis in *Arabidopsis*. Plant Cell **24:** 5007–5023.

Weber, H., Bernhardt, A., Dieterle, M., Hano, P., Mutlu, A., Estelle, M., Genschik, P., and Hellmann, H. (2005). *Arabidopsis* AtCUL3a and AtCUL3b form complexes with members of the BTB/POZ-MATH protein family. Plant Physiol. **137:** 83–93.

Weber, H., and Hellmann, H. (2009). *Arabidopsis thaliana* BTB/ POZ-MATH proteins interact with members of the ERF/AP2 transcription factor family. FEBS J. **276:** 6624–6635.

Woo, H.R., Kim, J.H., Kim, J., Kim, J., Lee, U., Song, I.J., Kim, J.H., Lee, H.Y., Nam, H.G., and Lim, P.O. (2010). The RAV1 transcription factor positively regulates leaf senescence in *Arabidopsis*. J. Exp. Bot. **61:** 3947–3957.

Yun, K.Y., Park, M.R., Mohanty, B., Herath, V., Xu, F., Mauleon, R., Wijaya, E., Bajic, V.B., Bruskiewich, R., and de Los Reyes, B.G. (2010). Transcriptional regulatory network triggered by oxidative signals configures the early response mechanisms of japonica rice to chilling stress. BMC Plant Biol. **10:** 16.

Zhang, W., Zou, A., Miao, J., Yin, Y., Tian, R., Pang, Y., Yang, R., Qi, J., and Yang, Y. (2011). LeERF-1, a novel AP2/ERF family gene within the B3 subcluster, is down-regulated by light signals in *Lithospermum erythrorhizon*. Plant Biol. (Stuttg.) **13:** 343–348.